Available online at www.sciencedirect.com
SCIENCE DIRECT®
Computers & Fluids 35 (2006) 920–924
computers & fluids
www.elsevier.com/locate/compfluid

Lattice kinetic simulations of 3-D MHD turbulence

G. Breyiannis *, D. Valougeorgis

Department of Mechanical and Industrial Engineering, University of Thessaly, Pedion Areos, Volos 38334, Greece

Received 29 July 2004; accepted 17 July 2005
Available online 10 January 2006

Abstract

A recently proposed lattice Boltzmann kinetic scheme offers a promising tool for simulating complex 3-D MHD flows. The algorithm is based on the BGK modeling of the collision term. The conventional approach for implementing magnetic behavior in LBM methods is based on one tensor-valued distribution function to present both the fluids variables (density and momentum) and the magnetic field. This formulation, however, has been proven a rather inefficient approach. The present scheme calls for a separate BGK-like evolution equation for the magnetic field which models the induction equation and enhances simplicity while allowing for the independent adjustment of the magnetic resistivity. Furthermore the algorithm correctly recovers the macroscopic dissipative MHD equations. Numerical results for the 3-D Taylor–Green vortex problem are presented with corresponding results computed with a pseudo-spectral code used as benchmark.

1. Introduction

Lattice Boltzmann methods (LBM) have proven to be an efficient alternative to classical CFD solvers in many areas of fluid flows [1,2]. Applications of the method range from particulate and multiphase flows to porous media and other complex flow systems. In general, LBM present superior ability in dealing with non-ideal fluids and complicated geometries. They present an effective framework in order to tackle physical phenomena that cannot be formulated in a comprehensive macroscopic description.

LBM focus on the proper time integration of the mesoscopic Boltzmann kinetic equation under specific constraints that reflect the macroscopic conservative processes. The corresponding macroscopic behavior is recovered at the long wave length limit. The explicit nature of the algorithm is amenable to high parallelization. Despite the significant advantages there are still unresolved problems such as a comprehensive thermal configuration, high Mach number flows and turbulence [2].

Magnetohydrodynamics, in the context of LBM, have initially utilized a tensor distribution function f_α^σ whose moments produced all the relevant macroscopic quantities. However this approach required the introduction of a second base vector for the discrete particle velocities [3]. Although there has been efforts to optimize the approach by reducing the complexity of the system, this formulation adds significant burden on the numerics suggesting a cumbersome extension to 3-D geometry [4].

Recently a new approach was presented by Dellar [5]. He argued that the evolution of the magnetic field can be formulated in terms of a kinetic BGK-type equation similar to Boltzmann's equation. Although there is no analogous microscopic process it can be seen [6] that any conservative hyperbolic system can be formulated in this way, under appropriate constraints. Thus, two distinct kinetic equations provide the needed macroscopic variables **u** and **B**.

The corresponding Lorentz force can be incorporated in two ways. Either with an a priori derivation of the extended Boltzmann equation to include an external acceleration term [7], on the left hand side of the Boltzmann equation, or via an extension to the equilibrium function

* Corresponding author.
E-mail address: gbregian@mie.uth.gr (G. Breyiannis).

0045-7930/$ - see front matter © 2005 Elsevier Ltd. All rights reserved.
doi:10.1016/j.compfluid.2005.07.016

[5], on the right hand side, one that correctly accounts for the modified stress due to the Lorentz force.

Here, following Dellar [5], we extend his treatment of the equilibrium function in 3-D and implement the discretization introduced in [7], in order to report results on the ability of kinetic schemes to simulate complex fully 3-D turbulent MHD flows. As a test case we consider a periodic cube with deterministic initial conditions.

2. Formulation

2.1. Hydrodynamic field

The numerical implementation of the method is based on the discretized Boltzmann equation with a BGK formulation of the collision term (LBGK), which takes the form

$$\partial_t f_i + \boldsymbol{\xi}_i \cdot \nabla f_i = -\frac{1}{\tau}(f_i - f_i^{(0)}) \tag{1}$$

where $f_i = f(\mathbf{x}, \boldsymbol{\xi}_i, t)$, with $\mathbf{x}$ the spatial vector, $\boldsymbol{\xi}_i$ the microscopic velocity set chosen, t the time and τ the relaxation time. All quantities are dimensionless unless otherwise stated. For the isothermal case, the equilibrium distribution function is given by a low Mach number series expansion of the Maxwellian as

$$f_i^{(0)} = \varrho w_i \left[1 + \frac{\boldsymbol{\xi}_i \cdot \mathbf{u}}{\theta} + \frac{(\boldsymbol{\xi}_i \cdot \mathbf{u})^2}{2\theta^2} - \frac{\mathbf{u} \cdot \mathbf{u}}{2\theta}\right], \tag{2}$$

with the weighting factors w_i depending on the lattice and $\theta = c_s^2$. In 3-D space, there are several lattice models that can be used for the hydrodynamic part of the problem, utilizing 15, 19 or 27 discrete velocity vectors. It has been seen that the 19-velocity lattice is efficient and stable enough to recover the correct hydrodynamic response of a 3-D flow [8]. We chose to perform our simulations with the 19-velocity model (Fig. 1(a)) incorporating $c_s = c/\sqrt{3}$ with $c = \delta x/\delta t$ being the lattice speed and corresponding weights,

$$w_i = \begin{cases} 1/3, & i = 0 \\ 1/18, & i = 1, \ldots, 6 \\ 1/36, & i = 7, \ldots, 18 \end{cases}$$

Following the standard practice in LBM, we set $\delta x = \delta t = 1$, postulating $c = 1$. The macroscopic quantities can be computed by moments of f, i.e. $\varrho = \sum_i f_i$ and $\varrho\mathbf{u} = \sum_i \boldsymbol{\xi}_i f_i$, where ϱ and $\mathbf{u}$ are the density and velocity vector, respectively and the viscosity of the fluid is given by $\nu = \tau c_s^2$.

2.2. Magnetic field

The evolution of a magnetic field follows an advection–diffusion equation that, in conservative form, can be formulated as

$$\partial_t \mathbf{B} + \nabla \cdot (\mathbf{uB} - \mathbf{Bu}) = \eta \nabla^2 \mathbf{B} \tag{3}$$

where η is the magnetic resistivity. Following the theoretical work of Bouchut [6], Dellar [5] suggested that a kinetic equation of BGK-type can be used to simulate the above equation in mesoscopic level as long as appropriate constraints are imposed to secure proper macroscopic behavior. It should be noted that there are no physical grounds to suggest that. The motivation stems from the fact that the macroscopic induction equation is similar to the Navier–Stokes momentum equation. However, unlike the momentum flux tensor which is symmetric, the corresponding electric field tensor is antisymmetric and thus cannot be formulated as the second moment of a single distribution function. The alternative is to use a vector distribution function with its zeroth moment providing the magnetic field vector,

$$\mathbf{B} = \sum_{j=0}^{M} \mathbf{g}_j. \tag{4}$$

The evolution of $\mathbf{g}_j$ obeys a BGK-type kinetic equation

$$\partial_t \mathbf{g}_j + \boldsymbol{\Xi} \cdot \nabla \mathbf{g}_j = -\frac{1}{\tau_m}\left(\mathbf{g}_j - \mathbf{g}_j^{(0)}\right) \tag{5}$$

where $\mathbf{g}_j^{(0)}$ are the corresponding equilibrium distribution functions given by

$$\mathbf{g}_{j\beta}^{(0)} = W_j\left[B_\beta + \Theta^{-1}\boldsymbol{\Xi}_{j\alpha}(u_\alpha B_\beta - B_\alpha u_\beta)\right] \tag{6}$$

with α, β denoting the spatial directions and $\boldsymbol{\Xi}$ the corresponding discrete velocity vector (not necessarily the same as $\boldsymbol{\xi}$). The relaxation time τ_m allows us to set the magnetic

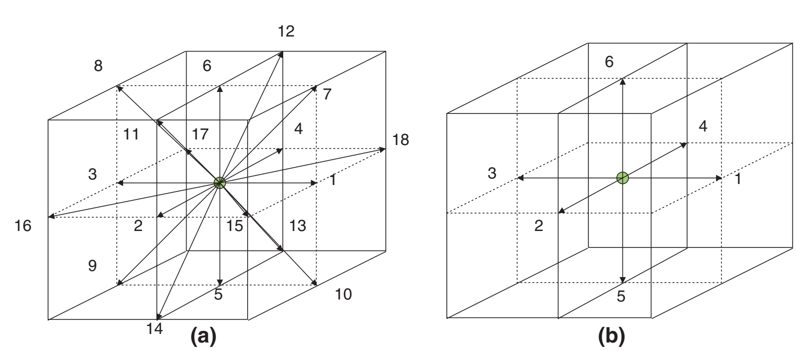

Fig. 1. Discrete velocity lattice for the (a) hydrodynamic (3DQ19) and (b) magnetic (3DM7) fields.

resistivity independently from the fluid's viscosity, which is related to τ.

The first moment of $\mathbf{g}$ gives the electric tensor as

$$\Lambda^{(0)}_{\alpha\beta} = \sum_{j=0}^{M} \Xi_{j\alpha} g^{(0)}_{j\beta} = u_\alpha B_\beta - B_\alpha u_\beta. \tag{7}$$

Note that we can also get consistent expressions for $\nabla \cdot \mathbf{B}$ and $\nabla \times \mathbf{B}$ [5].

Dellar [5] modeled the Lorentz force with an additional term in the equilibrium by expressing the Lorentz force as the divergence of the Maxwell stress tensor,

$$(\nabla \times \mathbf{B}) \times \mathbf{B} = \nabla \cdot \mathbf{M} = \nabla \cdot \left[\frac{1}{2}\delta_{\alpha\beta}|\mathbf{B}|^2 - B_\alpha B_\beta\right]. \tag{8}$$

This implies that the Euler momentum equation can be written as

$$\partial_t(\varrho\mathbf{u}) + \nabla \cdot \left(P\mathbf{I} + \varrho\mathbf{u}\mathbf{u} + \frac{1}{2}B^2\mathbf{I} - \mathbf{B}\mathbf{B}\right) = 0. \tag{9}$$

It can be seen that the Taylor expansion of the equilibrium function is equivalent to a moment expansion in tensor Hermite polynomials. This is evident if we write (2) as

$$f^{(0)} = w_i\left(\varrho + \frac{1}{\theta}(\varrho\mathbf{u}) \cdot \xi_i + \frac{1}{2\theta^2}[(P - \theta\varrho)\mathbf{I} + \varrho\mathbf{u}\mathbf{u}] : (\xi_i\xi_i - \theta\mathbf{I})\right). \tag{10}$$

Thus an extension to the equilibrium function can be given from

$$w_i \frac{1}{2\theta^2}(\xi_i\xi_i - \theta\mathbf{I}) : (\mathbf{M} - \theta\mathbf{I}(Tr\mathbf{M})), \tag{11}$$

where Tr stands for the trace of a matrix, with an error consistent with the truncation error [5]. In three dimensions and for $\theta = 1/3$ the above extension becomes

$$w_i \frac{9}{2}\left(\frac{1}{3}|\mathbf{B}|^2|\xi_i|^2 - (\xi_i \cdot \mathbf{B})^2\right). \tag{12}$$

Adding this component to the equilibrium function (2) would correctly, up to second moment, reproduce the macroscopic Euler MHD equations. Note that the extra term has the zeroth and first moment in terms of ξ equal to zero. Thus the macroscopic dissipative MHD equations are recovered at the hydrodynamic limit as

$$\partial_t(\varrho\mathbf{u}) + \nabla \cdot (P\mathbf{I} + \varrho\mathbf{u}\mathbf{u}) = (\nabla \times \mathbf{B}) \times \mathbf{B} + \nabla \cdot (2\nu\varrho\mathbf{S}), \tag{13}$$

with the strain tensor given by $\mathbf{S}_{\alpha\beta} = \frac{1}{2}(\partial_\alpha u_\beta + \partial_\beta u_\alpha)$.

The magnetic lattice has to retain a symmetry only up to third order. Thus significantly fewer discrete velocity vectors are required for accurate simulations. In the 3-D case a 7-velocity lattice is adequate. The corresponding weights in Eq. (6) are

$$W_0 = \frac{1}{4}, \quad W_j = \frac{1}{8} \quad \text{for} \quad j = 1, 2, 3, 4, 5, 6 \tag{14}$$

while $\Theta = 1/4$ and the magnetic resistivity is given as $\eta = \tau_m\Theta$. The above scheme maintains high accuracy in all times.

3. Algorithm

The time integration of (1) and (5) can be carried out to second order in δt by appropriate change of variables [2,5],

$$\overline{f_i}(x,t) = f_i(x,t) + \frac{\delta t}{2\tau}\left(f_i(x,t) - f_i^{(0)}(x,t)\right) \tag{15}$$

$$\overline{\mathbf{g}_j}(x,t) = \mathbf{g}_j(x,t) + \frac{\delta t}{2\tau_m}\left(\mathbf{g}_j(x,t) - \mathbf{g}_j^{(0)}(x,t)\right) \tag{16}$$

where one can compute the needed macroscopic quantities from moments of the barred functions.

Now the discretized evolution equations become

$$\overline{f_i}(x+\xi_i\delta t, t+\delta t) = \overline{f_i}(x,t) - \frac{\delta t}{(\tau + 0.5\delta t)}\left[\overline{f_i}(x,t) - f_i^{(0)}(x,t)\right] \tag{17}$$

$$\overline{\mathbf{g}}_j(x+\Xi_j\delta t, t+\delta t) = \overline{\mathbf{g}}_j(x,t) - \frac{\delta t}{(\tau_m + 0.5\delta t)}\left[\overline{\mathbf{g}}_j(x,t) - \mathbf{g}_j^{(0)}(x,t)\right] \tag{18}$$

with

$$f^{(0)} = \varrho w_i\left[1 + \frac{(\xi \cdot \mathbf{u})}{\theta} + \frac{(\xi \cdot \mathbf{u})^2}{2\theta^2} - \frac{\mathbf{u}^2}{2\theta}\right] + w_i\frac{9}{2}\left(\frac{1}{3}|\mathbf{B}|^2|\xi_i|^2 - (\xi_i \cdot \mathbf{B})^2\right) \tag{19}$$

and $\mathbf{g}^{(0)}$ given by (6).

The 7-velocity lattice (3DM7) used for the discretization of the magnetic field evolution is depicted in Fig. 1(b). The relations for viscosity and resistivity for the implemented lattices are $\nu = \tau/3$ and $\eta = \tau_m/4$, respectively.

Given the initial quantities of $\mathbf{u}$ and $\mathbf{B}$, we compute first the equilibrium distributions from (6) and (19), and then the right hand sides of (17) and (18), which represent the collision process. The next step includes the advection along the discrete velocity vector. Finally, we compute the new macroscopic quantities by the corresponding moments and so forth.

4. Results

We test the algorithm for a simplified problem of decaying isotropic turbulence in a 3-D cube with periodic boundary conditions. Our numerical results are compared with those of a pseudo-spectral code provided by Carati [9].

The configuration used as a prototype of MHD computations consists of an implementation of the Taylor–Green vortex [10] with a corresponding magnetic field. The initial conditions, in physical space, for the velocity and magnetic field are given by

$$\mathbf{u} = [\sin(x)\cos(y)\cos(z), -\cos(x)\sin(y)\cos(z), 0] \tag{20}$$

$$\mathbf{B} = [\sin(x)\sin(y)\cos(z), \cos(x)\cos(y)\cos(z), 0] \tag{21}$$

with $0 < x, y, z < 2\pi$. The kinetic and magnetic energies per unit volume are defined as

$$E_{\text{kinetic}} = \frac{1}{2L^3}\int |\mathbf{u}|^2 d\mathbf{x} \tag{22}$$

$$E_{\text{magnetic}} = \frac{1}{2L^3}\int |\mathbf{B}|^2 d\mathbf{x} \tag{23}$$

with the corresponding enstrophies given by

$$\Omega_{\text{kinetic}} = \frac{1}{2L^3}\int |\nabla\times\mathbf{u}|^2 d\mathbf{x} \tag{24}$$

$$\Omega_{\text{magnetic}} = \frac{1}{2L^3}\int |\nabla\times\mathbf{B}|^2 d\mathbf{x}. \tag{25}$$

with $L = 2\pi$. In all simulations viscosity and magnetic resistivity are set equal. The computer code implements mpi parallelization and simulations have been carried out in linux clusters.

A detailed comparison between the lattice kinetic scheme and the spectral method is shown in Figs. 2 and 3 where the temporal evolution of the kinetic and magnetic energies and their respective enstrophies are presented in dimensional units. The formula for the relaxation time is

$$\tau = \frac{UN}{\theta Re}, \tag{26}$$

where U is the lattice velocity, $\theta = 1/3$, N is the number of lattice units utilized and Re the Reynolds number of the flow. The spectral scheme utilized a 32^3 mesh while the LBGK simulation used $N = 103$ with $Ma = U/c_s = 0.061\sqrt{3}$. The need for higher resolutions for the LBM simulations is due to the formulation of the scheme. It is known that small values of τ are troublesome in simulations, thus for high Re, and low Mach number, one must increase N to achieve stability, limited only by available resources. Three sets of results are given for $\nu = \eta$ equal to 0.1, 0.05 and 0.01. The nominal Reynolds number is $Re = 2\pi/\nu$ and the dimensional time plotted in Figs. 2 and 3 is computed as $t = \frac{2\pi U}{N} n_t$, where n_t is the number of iterations.

The results in Figs. 2 and 3 reproduce the well known mechanism of energy transfer between magnetic and hydrodynamic parts as the Reynolds number increases while at the same time the dissipation rate is noticeably enhanced through the creation of currents and vorticity sheets [11]. It is seen that there is an excellent quantitative agreement between the results of the implemented magnetohydrodynamic lattice kinetic scheme and those of the pseudo-spectral method. The spectral approach is arguably more computationally efficient at this range of the Reynolds number. However as the complexity of the flow increases the grid requirements posed by the flow field should meet those needed by the kinetic scheme. Then, the superior ability of the LBM in terms of parallel

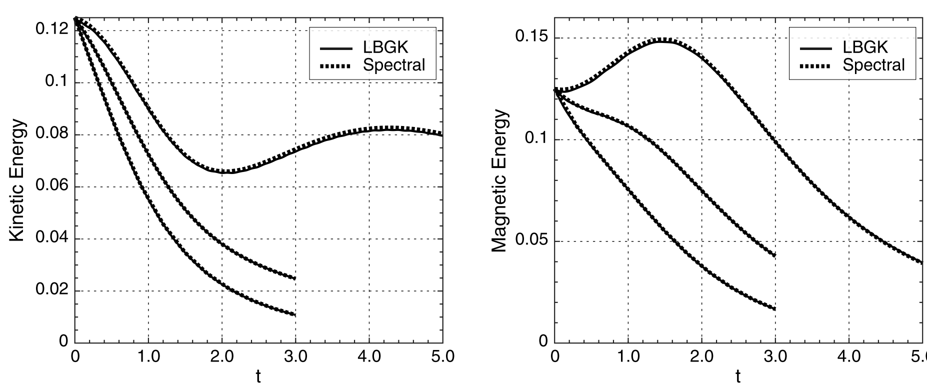

Fig. 2. Temporal evolution of kinetic and magnetic energies for $\nu = \eta = 0.1$, 0.05, 0.01 (bottom line to top line).

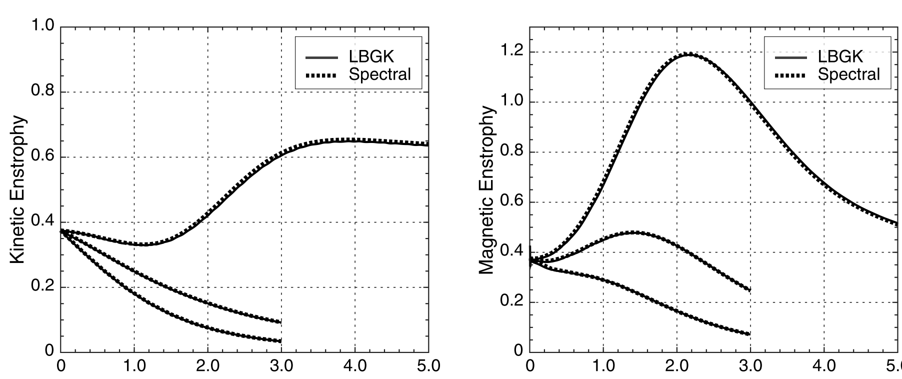

Fig. 3. Temporal evolution of kinetic and magnetic enstrophies for $\nu = \eta = 0.1$, 0.05, 0.01 (bottom line to top line).

programming and handling boundary conditions will bear fruits.

5. Conclusion

Lattice kinetic simulations of 3-D homogeneous MHD turbulence have been carried out. The configuration consists of a periodic cube with deterministic initial conditions for the velocity and magnetic field. The results indicate the existence of a complex evolution through nonlinear interaction between current and vorticity. A fine quantitative agreement with spectral simulations is found for the cases tested here. A more detailed and time demanding comparison study for high Reynolds number flows is currently under way. These results suggest that lattice kinetic schemes can handle 3-D MHD flows, such as those related to fusion plasma research.

Acknowledgements

Partial support for this work by the Euratom–Hellenic Republic Association, is gratefully acknowledged. We would also like to thank Prof. D. Carati for providing the spectral code and Prof. Krafczyk for the use of his computational facilities.

References

[1] Chen S, Doolen GD. Lattice Boltzmann method for fluid flows. Annu Rev Fluid Mech 1998;30:329.

[2] Nourgaliev RR, Dinh TN, Theofanous TG, Joseph D. The lattice Boltzmann equation method: theoretical interpolation, numerics and implications. Int J Mult Flow 2003;29:117.

[3] Martínez DO, Chen S, Matthaeus WH. Lattice Boltzmann magnetohydrodynamics. Phys Plasmas 1994;1:1850.

[4] Macnab A, Vahala G, Vahala L, Pavlo P, Soe M. Some progress in the development of lattice Boltzmann methods for dissipative MHD. Czech J Phys 2002;52.

[5] Dellar PJ. Lattice kinetic schemes for magnetohydrodynamics. J Comput Phys 2002;179:95.

[6] Bouchut F. Construction of BGK models with a family of kinetic entropies for a given system of conservation laws. J Stat Phys 1999;95:113.

[7] Breyiannis G, Valougeorgis D. Lattice kinetic simulations in 3-D magnetohydrodynamics. Phys Rev E 2004;69:065702.

[8] Mei R, Shyy W, Yu D, Luo L-S. Lattice Boltzmann method for 3-D flows with curved boundary. J Comput Phys 2000;161:680.

[9] D. Carati, Université Libre de Bruxelles, Association EURATOM-Etat Belge, personal communication.

[10] Brachet ME, Meiron DI, Orszag SA, Nickel BG, Morf RH, Frisch U. Small-scale structure of the Taylor–Green vortex. J Fluid Mech 1983;130:411.

[11] Davidson PA. An introduction to magnetohydrodynamics. Cambridge University Press; 2001.